

Visualizing Black Holes and Gravitational Collapse with Digital Holography

Rob Hocking¹ and Loïc Chérél²

¹Taiwan; rob.l.hocking@gmail.com, ²France; loic74650@gmail.com

Abstract

In recent years, digital holography has progressed to a level of realism where humans fail to distinguish holograms from reality. Our goal in this work is to apply this technology to the visualization of both static black holes and the dynamic collapse of a ball of dust into a black hole. While the former has been done, to the best of our knowledge, it has never been done using holography—whereas the latter appears never to have been done at all. Different options for producing the hologram are compared.



Figure 1: Stereo pair of a black hole hologram. Cross your eyes using the technique [1] to view in stereo 3D.

Introduction

Black hole visualization is not new, with the earliest work done in the late 70s [16]. In 2014, the film *Interstellar* made it mainstream with the spectacular and mostly scientifically accurate rendering of the black hole Gargantua. Given the wealth of visualizations out there, why create more?

There are really two answers to this question. Firstly, the content out there is quite limited from a technological perspective—most of it is just animations, and not even stereo 3D ones. Secondly, the overwhelming majority are visualizations of simple static black holes, while visualizations of more interesting and computationally challenging scenarios are mostly non-existent. In particular, visualizations of the dynamic formation of a black hole by means of gravitational collapse (of particular interest in this paper) are nowhere to be found. To be a bit more precise, visualizations of *what the human eye would see* appear to be non-existent—other types of visualization may be found, see for example [2], but they tend to be animated graphs that are difficult for a non-specialist to understand.

On the other hand, popular science books are full of descriptions of what gravitational collapse would look like. For example, *A Brief History of Time* [13, p. 47] describes the process like this (we have paraphrased for brevity):

“To understand what you would see if a star collapsed into a black hole, remember that in relativity there is no absolute time. Imagine an astronaut on the star’s surface, falling inward as it collapses, sending a signal every second to a spaceship in orbit. At some point on his watch—say 11:00—the star shrinks below the critical radius where its gravity is so strong that nothing can escape, and his signals no longer reach the spaceship.

As 11:00 approaches, the intervals between signals lengthen from the perspective of the orbiting observers. They wait only slightly more than a second for the 10:59:58 and 10:59:59 signals, but they wait forever for the 11:00 signal. Any light emitted between 10:59:59 and 11:00 is stretched out over an infinite period, making the star’s glow appear ever redder and dimmer. Eventually, it becomes too faint to detect, leaving only a black hole in its place.”

Our aim in this paper is twofold. Firstly, it is to apply to black hole visualization digital holography, a visualization technique so realistic that humans fail tests to correctly distinguish holograms from reality [10]. Secondly, it is to do the math required to turn the quotation above into a scientifically accurate visualization, and to build from that a digital hologram.

A hologram is typically mounted within a picture frame and looks like a window into a 3D scene that can either be fully behind the window or partially in front of it. That is, the objects contained within a hologram look fully 3D (without the need for special glasses or other equipment) and move when you do, just like in the case of a real window with a real 3D scene behind it. Holograms can be either analog or digital. In the analog case, you need to be able to interact with a real, physical copy of the 3D object in order to make the hologram. The closest known black hole to earth is Gaia BH1 and is located roughly 1,560 light years away, so analog is out. On the other hand, to make a digital hologram all you need is the ability to render a virtual 3D scene from a sufficiently large number of angles. Hence we have gone the digital route.

It was not a priori obvious that black holes would work in stereo 3D. It could have been the case that gravitational lensing would warp the environment of a black hole so much that our brains would be too confused to make sense of a stereo pair. This would have killed the project, as black holes working in stereo 3D is a precondition for them working as holograms. Fortunately, Figure 1 shows that they do work.

Due to the enormous expense and difficulty in creating a digital hologram printer, most digital holographers can only get their holograms made by paying either Geola or Ultimate Holography, the two main digital hologram manufacturers in the world today, to do it for them. Note that the holograms produced by Ultimate Holography are called “Chimera holograms” and will be referred to as such in the text. However, one of us (Loïc) is currently developing such a printer and is open to testing various hologram printing techniques. In this work, we produce holograms both using his printer, and using the printing services above.

A Brief Explanation of Digital Holograms and how to Make Them

In the absence of obstacles (and in flat spacetime), the color visible to the eye in direction \vec{v} is constant along a line parallel to \vec{v} . This motivates the concept of a *light field*, which is the assignment of a color to every line in \mathbb{R}^3 [15]. Digital holograms work based on the observation that if you can reconstruct at the surface \mathcal{H} of a hologram the light field of a virtual 3D scene restricted to \mathcal{H} , the result is visually indistinguishable from a window into a virtual world containing the 3D scene, even as one changes one’s viewing angle.

To achieve this, digital holograms are divided up into a large number of “hogels” or “holographic pixels”. Unlike regular pixels, which are tiny light sources giving off the same color of light in every direction, hogels may be thought of as tiny light sources giving off *different* colors of light in different directions. In the limit where there is a hogel at every point \vec{p} on \mathcal{H} , and said hogel assigns a different color to every direction \vec{v} coming out of \vec{p} , the light field may be reconstructed. A digital hologram is thus defined by a mapping $\vec{C}(\vec{p}, \vec{v})$ assigning a color to every point \vec{p} on \mathcal{H} and every direction \vec{v} coming out of \vec{p} . In practice, the

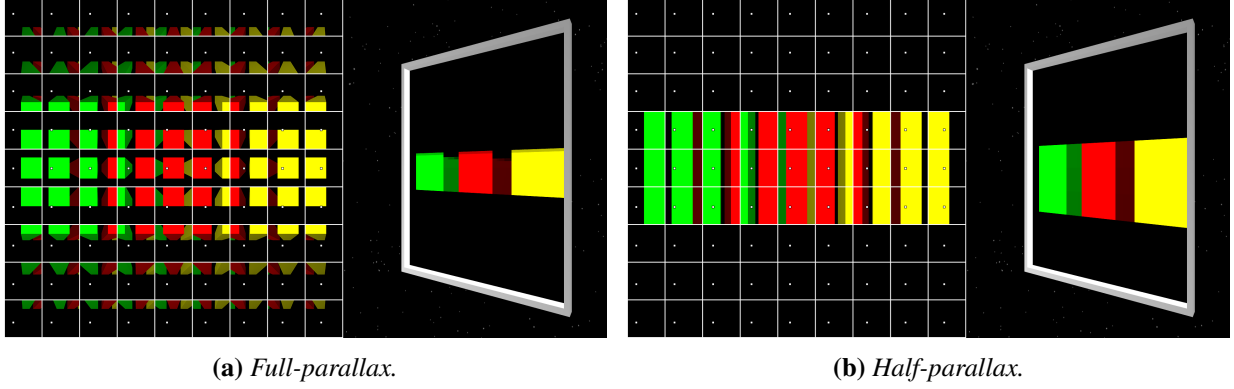


Figure 2: Illustration of half- and full-parallax holograms of a simple 3D scene (three boxes), rendered using a 9×9 grid of hogels. The hogels and their associated hogel images are illustrated on the left of each subfigure, while the simulated hologram view is on the right. The white dot in each hogel image represents the current direction from which we are viewing the hologram.

mapping \vec{C} is restricted to a discrete grid of hogels $\{\vec{p}_{a,b}\}$ and a finite set of directions $\{\vec{v}_{i,j}\}$. For each fixed $\vec{p}_{a,b}$, \vec{C} is represented by means of a “hogel image” encoding which colors are emitted by the hogel in a discrete set of directions $\{\vec{v}_{i,j}\}$.

To make this concrete, let’s suppose our 3D scene consists of three boxes (green, red, and yellow) that we want to appear *behind* the hologram, and that we are using a 9×9 grid of hogels, each of which has a 100×100 pixel hogel image. In Figure 2(a)-(b) we have actually done this, with the 9×9 grid of hogel images on the left of each subfigure and a simulation of the resulting hologram on the right. The white dot (let’s call it the “focus region”) in each hogel image is essentially the current viewing direction - a hologram viewed from a fixed direction is generated using only the portions of each hogel image corresponding to said direction (i.e. underneath the “focus region”). When you change your viewing direction, the focus regions move and the appearance of the hologram changes. Please see the supplementary material for an animation of this and a clearer explanation than we can give in writing.

An important concept in digital holography is the distinction between *half-parallax* and *full-parallax* holograms. In a nutshell, the 3D-scene in a full-parallax hologram moves with your head regardless of the direction in which your head moves. However, half-parallax holograms only respond to horizontal changes. They necessarily have hogel images that are constant in the y-direction. This is illustrated in Figure 2(b). This shouldn’t be surprising as vertical motions of your head correspond to vertical motions of the focus region, which needs to always see the same color for the hologram to not change appearance.

When you make a digital hologram using a manufacturer such as Geola or Ultimate Holography, you do not generate the hogel images yourself. Rather, you give them a set of renderings of your 3D scene from a dense grid of camera positions on a “camera surface” C . Effectively, you are specifying the light field on C , rather than on \mathcal{H} . They then infer the hogel images by calculating the light field on \mathcal{H} given its values on C . If you only want to generate a half-parallax hologram, it is sufficient to provide renderings along a 1D “camera arc” C . The Chimera holograms (holograms produced by Ultimate Holography) in this paper are half-parallax; the information we provided to Ultimate Holography in order to generate them was a set of 1200 renderings along an 180° circular arc centered on the black hole with the camera looking towards it.

On the other hand, for Loïc’s printer we generated the hogel images directly ourselves. We also did the computations necessary to generate full-parallax holograms. Each full-parallax hologram required the computation of over 33,000 hogel images and took over ten days of computation time.

Spatio-Temporal Composition in Digital Holography

If a digital hologram is a window into a virtual 3D scene—and if that scene is *static*—then one might naturally wonder how a dynamic process such as gravitational collapse can be visualized using a single hologram (a stated goal of this project).

The answer is that there is no rule stating that a hologram must reveal the same 3D scene when viewed from every angle. One can, for example, have an animated scene with time beginning in the leftmost view (say) and ending in the rightmost view. One could even have multiple unrelated scenes all baked into the same hologram, each with their own distinct viewing zone [7]. This is sometimes referred to as spatio-temporal composition and is an effect difficult to achieve in any other static medium [6].

We visualize the dynamics of gravitational collapse with time increasing as one moves from the leftmost view of the hologram, where one sees only mild distortion, to the rightmost view, where one sees the fully formed black hole. Intermediate views show intermediate stages of collapse. Since one's left and right eyes see the hologram at different horizontal angles and hence different moments in time, care must be taken to ensure that the change is not so rapid as to break the illusion of stereo 3D.

Rendering in Curved Spacetime

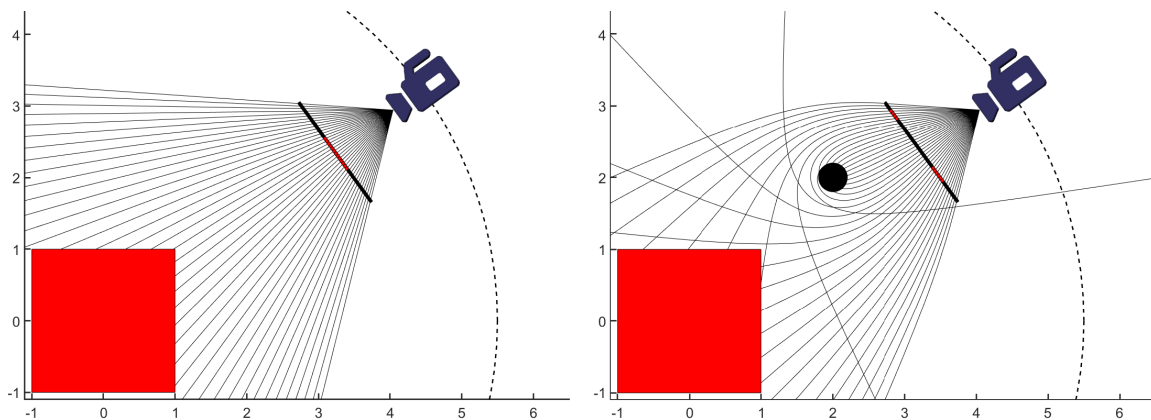


Figure 3: *Illustration of linear (left) vs. nonlinear (right) raytracing. Since light rays moving in the vicinity of a black hole follow curved geodesics, black hole visualization requires the latter.*

Provided they are far enough away from other matter, black holes are visible only because they bend the light passing by them. This makes rendering them something of a challenge—to the best of our knowledge, it is not possible to render one within a standard rendering engine like 3D Studio Max or Blender. You need to use a raytracer, and you need to modify it so that the rays move along curved trajectories defined by the geodesic equations of the black hole. This is called nonlinear ray tracing and is illustrated in Figure 3. We will not go into the details here other than to say that nonlinear raytracing has been well understood for decades and is straightforward to implement, and to provide the following reference [11].

Accurate shading is a much thornier issue. In flat spacetime, the typical approach in a raytracer is to find the straight line joining a point to be shaded with a light, and then to shade based on the distance to the light and the angle with which the light ray strikes the surface. This becomes enormously more complex when one is dealing with a black hole because:

1. Finding a light ray connecting two points in a black hole spacetime is non-trivial.
2. It turns out that there are typically infinitely many such light rays.

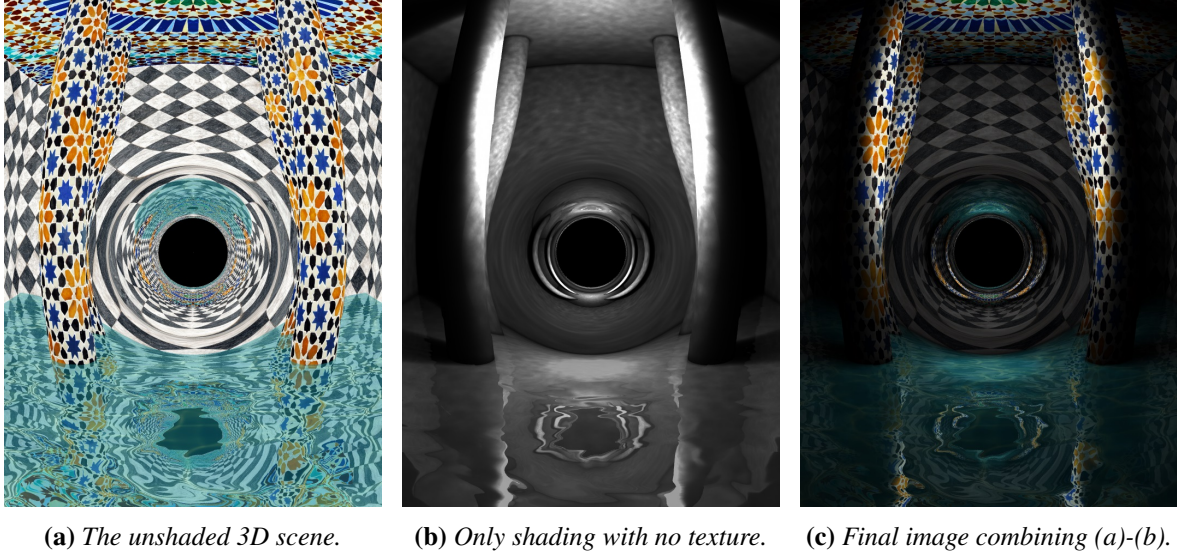


Figure 4: Rendering a black hole using nonlinear raytracing and nonlinear photon mapping.

To handle this, we decided to use a nonlinear variant of the photon mapping [14] algorithm. In brief, photon mapping works by shooting a large number of light rays from each light in a 3D scene into its environment, and keeping track of where they land. When shading a point, one then simply counts how many photons have landed “nearby”. This approach is readily adapted to curved light rays and neatly sidesteps the issues above.

Digital holograms suffer from increasing blur with distance from the hologram plane, making it difficult to depict scenes with significant depth [4, Ch. 11]. It was therefore necessary to place the black hole in a small enclosed space. We chose one loosely inspired by the Basilica Cistern in Istanbul. There is no artistic significance to this choice; it merely meets the conditions above while maintaining aesthetic appeal. In Figure 4 we illustrate the result with texture but no shading, shading but no texture, and the combination of both.

Oppenheimer-Snyder Gravitational Collapse

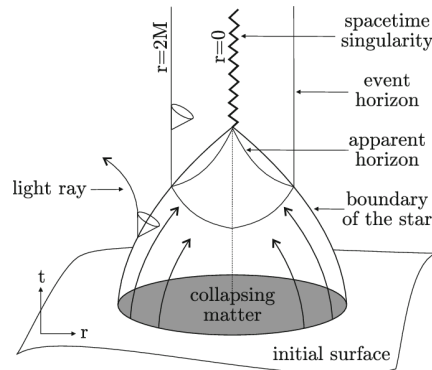


Figure 5: Spacetime diagram of the Oppenheimer-Snyder solution. Image credit: Figure 2 in [8].

On September 1, 1939—the same day Germany invaded Poland—Oppenheimer and his student Snyder published a paper presenting an analytical solution to Einstein’s equations of General Relativity. As illustrated in Figure 5, a ball of dust collapses under its own gravity, ultimately forming a black hole. Although largely ignored at the time, the paper was in retrospect a turning point for black hole physics. Oppenheimer had

paved the way for the physics community to accept black holes as real astronomical objects (namely, the final remnants of a dying star) rather than mere mathematical curiosities [3, p. 89].

The Oppenheimer-Snyder solution [17] gives us the mathematical machinery needed to turn Stephen Hawking’s high-level description into a scientifically precise visualization. The solution is defined in a piecewise manner, depending on whether you are inside or outside the ball of dust. Outside, it reduces to the 1916 Schwarzschild solution describing a static, spherically symmetric, uncharged, and non-rotating black hole [18]. Inside, it reduces to the 1922 closed FLRW solution describing a “big crunch” universe that collapses to a singularity in finite time [9]. The two solutions are seamlessly stitched together at the boundary of the dust cloud. However, each region is described using its own distinct coordinate system.

To simulate the appearance of Oppenheimer-Snyder gravitational collapse, numerically calculated light rays sent backward in time from the observer’s eye must seamlessly transition between these two coordinate systems every time a crossing event is detected. This must be done with great care, or else a seam will be visible in the calculated image.

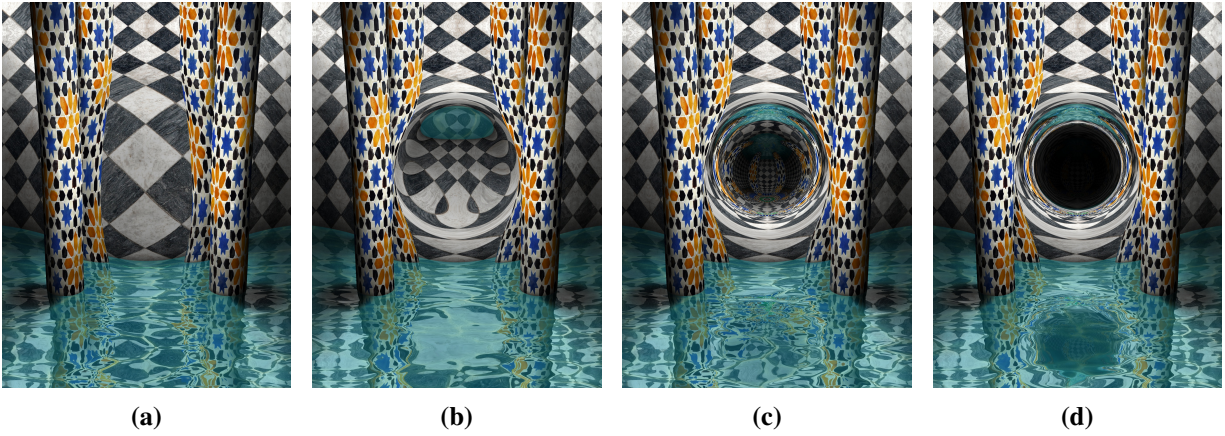


Figure 6: Four stages of Oppenheimer-Snyder gravitational collapse—time increases from left to right.

If the observer is at a point in time after which the black hole has formed, light rays directed backward in time from their eyes towards the black hole event horizon will “get stuck” there—continuing to travel backwards in time but essentially frozen in space. They only become “unstuck” when they have reached a time earlier than the time t_f at which the black hole forms. They are then free to enter the dust cloud, exit it on the other side, and eventually reach the place from which they were emitted in the distant past. Let’s call the emission time t_e and the time of arrival at the observer’s eye t_a . These rays have their brightness reduced by a factor of dt_e/dt_a . The emission t_e is determined primarily by t_f , as this is when the rays become “unstuck”, and it is asymptotically independent of t_a for $t_a \gg t_f$. Hence $dt_e/dt_a \rightarrow 0$ and the black hole dims and turns black.

Figure 6 shows the results of the simulation at four stages of evolution. In Figure 6(a), the dust is relatively dispersed, but dense enough to cause a modest bulging-type distortion. A short while later in Figure 6(b), the dust is concentrated enough to induce a highly distorted circular region, but without any visible darkening. Next, in Figure 6(c), the black hole is starting to take on its characteristic shape and significant darkening is apparent. Finally, in Figure 6(d), the black hole is almost fully formed and is distinguishable from an eternal Schwarzschild black hole only in that the dark circular region is not quite 100% black.

Results

We printed both the static black hole from Figure 4 and the dynamic Oppenheimer-Snyder collapse illustrated in Figure 6 using all three of Ultimate Holography (which *produces* Chimera holograms), Geola, and Loïc’s

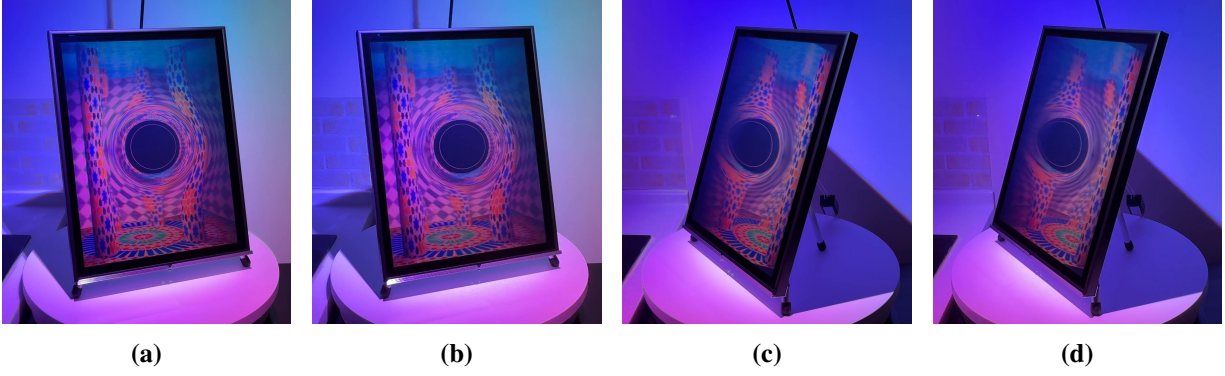


Figure 7: *Stereo pairs of the static black hole hologram. (a)-(b) form one pair while (c)-(d) form a second. Cross your eyes using the technique [1] to view in stereo 3D.*

printer. The Chimera and Geola holograms are quite large and so we limited ourselves to half-parallax (full-parallax is difficult at that size). On Loïc's printer we printed much smaller holograms in full-parallax.

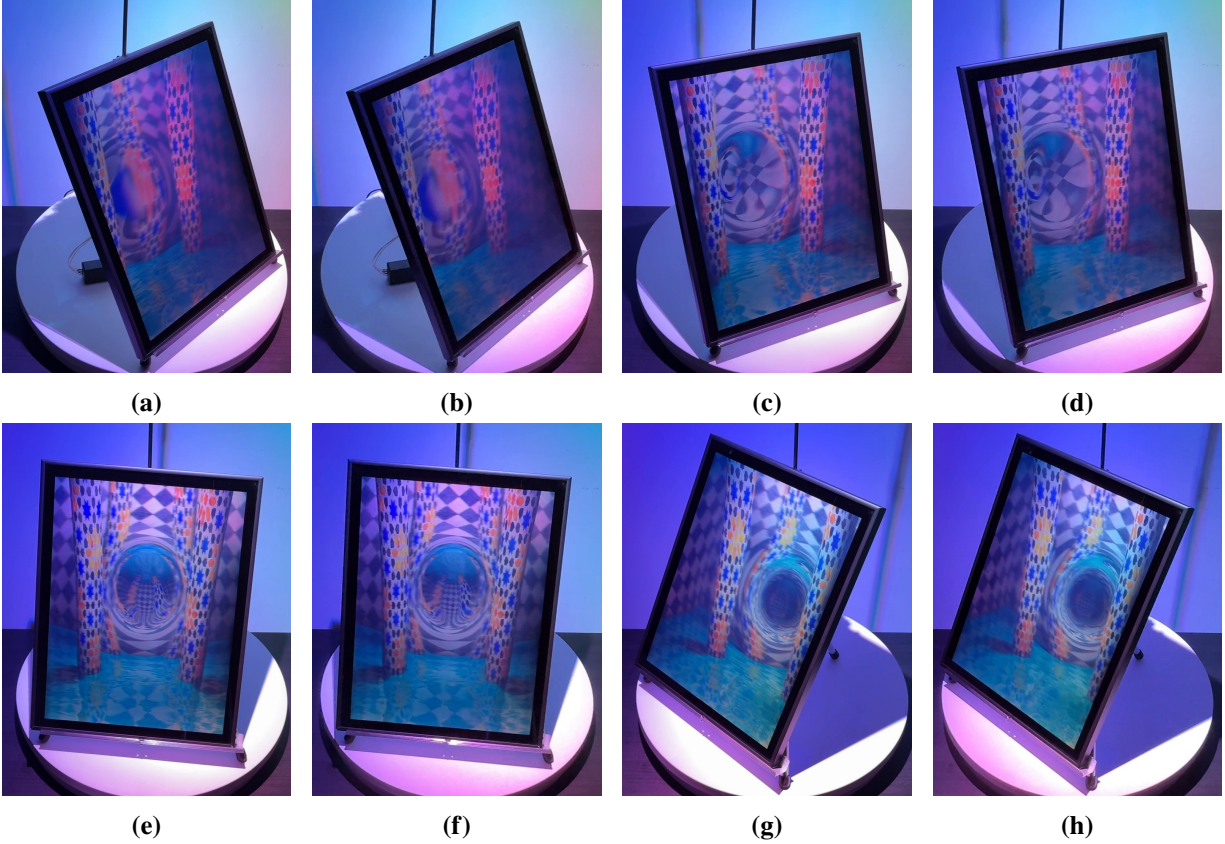


Figure 8: *Stereo pairs for the Oppenheimer-Snyder gravitational collapse hologram. Time increases as the hologram rotates, so that (a)-(b) form one stereo pair early in the collapse process, (c)-(d) and (e)-(f) are stereo pairs at intermediate times, and (g)-(h) is a stereo pair late in the process.*

Figure 7 provides stereo pairs of the static black hole hologram from a few angles, while Figure 8 does the same for Oppenheimer-Snyder collapse. Here we show only the Chimera holograms. For images and videos including the holograms printed on Loïc's printer and the Geola prints, see the supplementary material.

Conclusions and Future Work

In this work, we have created digital holograms visualizing both a static black hole and the dynamic formation of a black hole from a collapsing ball of dust. The former visualization has been done many times, but to our knowledge never as a hologram. The latter visualization seems to have never been done at all.

In the future, it would be interesting to create holograms of other gravitational phenomena. In particular, we originally intended to visualize gravitational collapse of a massless scalar field as studied by Matt Choptuik and others in the nineties [5, 12], which exhibits richer structure than the simpler Oppenheimer-Snyder model. However, upon reflection, we felt this would be unfair to Oppenheimer, who is remembered for his work on the atomic bomb but whose contributions to black hole physics are too often forgotten.

References

- [1] 3D without glasses, Cross-Eye HD. <https://www.youtube.com/watch?v=zBa-bCxsZDk>.
- [2] “SXS: Simulating eXtreme Spacetimes.” <https://www.black-holes.org/>. Accessed: January 28, 2025.
- [3] K. Bird and M. J. Sherwin. *American Prometheus: The Triumph and Tragedy of J. Robert Oppenheimer*, 2023rd ed. New York: Vintage, 2023.
- [4] D. Brotherton-Ratcliffe. *Ultra-Realistic Imaging - Advanced Techniques in Analogue and Digital Colour Holography*. 05 2013.
- [5] M. W. Choptuik. “Universality and scaling in gravitational collapse of a massless scalar field.” *Phys. Rev. Lett.*, vol. 70, Jan 1993, pp. 9–12. <https://link.aps.org/doi/10.1103/PhysRevLett.70.9>.
- [6] J. Desbiens. “Nomadic Perspectives: Spatial Representation in Oriental Scroll Painting and Holographic Panoramagrams.” vol. 4270. 10 2006. pp. 504–513.
- [7] J. Desbiens. “Experiments in image composition for synthetic holography.” 07 2009.
- [8] D. Dey and P. Joshi. “Gravitational collapse of baryonic and dark matter.” *Arabian Journal of Mathematics*, vol. 8, 04 2019.
- [9] A. Friedmann. “Über die Krümmung des Raumes.” *Zeitschrift für Physik*, vol. 10, Jan. 1922, pp. 377–386.
- [10] P. Gentet and S.-H. Lee. “True holographic ghost illusion.” *Opt. Express*, vol. 30, no. 15, Jul 2022, pp. 27 531–27 538. <https://opg.optica.org/oe/abstract.cfm?URI=oe-30-15-27531>.
- [11] E. Gröller. “Nonlinear ray tracing: Visualizing strange worlds.” *The Visual Computer*, vol. 11, 1995, pp. 263–274. <https://api.semanticscholar.org/CorpusID:16154056>.
- [12] R. S. Hamade and J. M. Stewart. “The Spherically symmetric collapse of a massless scalar field.” *Class. Quant. Grav.*, vol. 13, 1996, pp. 497–512.
- [13] S. W. Hawking. *A Brief History of Time*. New York: Bantam Books, 1988.
- [14] H. W. Jensen. “Realistic Image Synthesis Using Photon Mapping.” 2001. <https://api.semanticscholar.org/CorpusID:116917510>.
- [15] M. Levoy and P. Hanrahan. “Light field rendering.” *Proceedings of the 23rd annual conference on Computer graphics and interactive techniques*, 1996. <https://api.semanticscholar.org/CorpusID:1363510>.
- [16] J. P. Luminet. “Image of a spherical black hole with thin accretion disk.” , vol. 75, May 1979, pp. 228–235.
- [17] J. R. Oppenheimer and H. Snyder. “On Continued Gravitational Contraction.” *Phys. Rev.*, vol. 56, Sep 1939, pp. 455–459. <https://link.aps.org/doi/10.1103/PhysRev.56.455>.
- [18] K. Schwarzschild. “Über das Gravitationsfeld eines Massenpunktes nach der Einsteinschen Theorie.” *Sitzungsberichte der Königlich Preussischen Akademie der Wissenschaften*, Jan. 1916, pp. 189–196.